J. Fluid Mech. (1994), *vol.* 270, *pp.* 331–347

Evolution of disturbances in stagnation-point flow

By W. O. CRIMINALE,[1] T. L. JACKSON[2] AND D. G. LASSEIGNE[3]

[1] Department of Applied Mathematics, University of Washington, Seattle, WA 98195, USA

[2] Institute for Computer Applications in Science and Engineering, NASA Langley Research Center, Hampton, VA 23681, USA

[3] Department of Mathematics and Statistics, Old Dominion University, Norfolk, VA 23529, USA

(Received 10 August 1993 and in revised form 12 January 1994)

The evolution of three-dimensional disturbances in an incompressible three-dimensional stagnation-point flow in an inviscid fluid is investigated. Since it is not possible to apply classical normal-mode analysis to the disturbance equations for the fully three-dimensional stagnation-point flow to obtain solutions, an initial-value problem is solved instead. The evolution of the disturbances provides the necessary information to determine stability and indeed the complete transient as well. It is found that when considering the disturbance energy, the planar stagnation-point flow, which is independent of one of the transverse coordinates, represents a neutrally stable flow whereas the fully three-dimensional flow is either stable or unstable, depending on whether the flow is away from or towards the stagnation point in the transverse direction that is neglected in the planar stagnation point.

1. Introduction

Previous analytical work investigating the stability of planar stagnation-point flows has concentrated on the mathematical simplification provided by classical mode analysis of streamwise disturbances. Wilson & Gladwell (1978) have shown that incompressible planar stagnation flow is always stable to three-dimensional normal-mode self-similar disturbances that decay exponentially outside the viscous boundary layer. Lyell & Huerre (1985) re-examined the planar stagnation flow problem by using the same class of disturbances and verified the results of Wilson & Gladwell. They also characterized the other stable eigenvalue branches by showing that, after the initial branch found by Wilson & Gladwell, the other branches come in pairs. In addition, by a nonlinear analysis using a Galerkin method, Lyell & Huerre indicated that this same flow is unstable for disturbances of sufficiently high amplitude. On the other hand, a numerical study by Spalart (1989) found no such instability, suggesting that this was not the case. Brattkus & Davis (1991) showed that the normal-mode self-similar disturbances were the least stable of the class of disturbances that have a power-like behaviour in the downstream coordinate.

Lasseigne & Jackson (1992) allowed for density variations induced by a temperature difference between the free stream and the plate and determined that the stagnation flow remained stable to small streamwise disturbances regardless of the plate temperature. The effect of cooling the plate was to decrease the decay rate (less stable) of the small-wavelength disturbances while increasing the decay rate (more stable) of the moderate wavelengths. Again, only three-dimensional normal-mode self-similar disturbances that decay exponentially outside the viscous boundary layer were considered. Studies dealing with the swept attachment line also concentrated on streamwise normal-mode linear disturbances. Hall, Malik & Poll (1984) determined that a region of instability (in frequency–wavenumber space) associated with increasing crossflow exists. In independent investigations Kazakov (1991) and Lasseigne, Jackson & Hu (1992) determined the effects of surface temperature variations on this region of instability; the latter investigation also allowed for the effects of suction or blowing at the surface.

It is not possible to analyse the stability of the fully three-dimensional stagnation-point flow using normal-mode streamwise disturbances since the disturbance equations do not admit this class of disturbances as an eigenvalue problem. Therefore, the approach taken in this investigation is different than that of previous investigations. A more general initial value problem is solved using the methodology developed in Criminale & Drazin (1990) and has its origins in the work of Kelvin (1887) and Orr (1907*a*, *b*). The disturbances are taken to be initially bounded in all directions and the evolution of initial conditions is determined analytically and in closed form. By concentrating on the mean flow subject to disturbances in an inviscid fluid, the fully three-dimensional stagnation-point flow can be solved with the planar stagnation-point flow as a special case.

The method of analysis utilizes a moving coordinate transformation that allows easy integration (in time) of the individual vorticity components. Then, the double Fourier transform in the new transverse coordinates is used to reduce the mathematical problem to the solution of ordinary differential equations in which time appears strictly as a parameter. Thus, a completely analytical solution is found to the initial value problem describing the evolution of three-dimensional disturbances in three-dimensional stagnation-point flow in an inviscid fluid. The time evolution of a single Fourier mode in which the disturbance is periodic in the transverse directions is investigated in detail as well as the evolution of an initially localized disturbance. In both cases, the evolution of the total energy of the disturbance is used to illustrate the importance of the transient. Kelvin (1887) and Orr (1907*a*, *b*) have shown for different flow configurations that there can be growth in the perturbation energy even when the classical mode analysis shows that the flow is stable for long times.

Farrell (1989) applied this approach to two-dimensional disturbances within a two-dimensional counterflow as a good approximation to the local flow in regions of confluence and diffluence. It was determined that plane wave disturbances with dependence in the transverse coordinate and independent of the other coordinate have energy that grows exponentially in time. Plane wave disturbances with dependence in both coordinates experience an initial exponential growth, but eventually decay as time progresses. Disturbances with finite wave trains that were not spatially symmetric were shown to be stable but these disturbances also experienced an initial transient growth in energy with the energy asymptotically approaching a constant amplitude. Symmetric finite-wave-train disturbances were shown to not experience the initial transient growth and to have energy constant in time. This was seen to occur in regions of both confluence and diffluence.

The governing equations for the three-dimensional stagnation-point flow, the moving coordinate transformation and the linear disturbance equations are presented with the disturbance equations solved by the use of Fourier transforms in the transverse coordinates. Selected results for the evolution of a single Fourier mode are given in §3 and, in §4, results pertaining to the time evolution of a finite wave train described by an initially Gaussian profile are presented. In §5, a constant-pressure boundary condition is considered as an alternative to the zero normal velocity condition. Section

6 contains a discussion on the effects of background rotation and particle paths. Conclusions are given in §7.

2. Problem statement and basic equations

The problem under investigation is that of linearized disturbances in a three-dimensional stagnation-point flow. The basic flow is given non-dimensionally by

$$U = x, \quad V = -(1+\lambda)y, \quad W = \lambda z, \tag{1}$$

where λ is a measure of three-dimensionality. For $\lambda = 0$ the flow is a two-dimensional stagnation-point flow; for $\lambda = 1$ the flow is axisymmetric; for $-0.4294 < \lambda < 0$ the flow corresponds to two symmetrically displaced protuberances (Davey 1961), as displayed in figure 1. For $\lambda < 0$, it is important to observe that the flow is toward the stagnation point in the z-direction and away from the stagnation point in the x-direction. In addition, Davey has shown that separation occurs at $\lambda = -0.4294$, reversed flow exists for $-1 \leqslant \lambda < 0.4294$, and no solutions are possible for $\lambda < -1$.

The non-dimensional linearized equations for small disturbances are written as

$$u_x + v_y + w_z = 0, \tag{2a}$$

$$u_t + xu_x - (1+\lambda)yu_y + \lambda z u_z + u = -p_x, \tag{2b}$$

$$v_t + xv_x - (1+\lambda)yv_y + \lambda z v_z - (1+\lambda)v = -p_y, \tag{2c}$$

$$w_t + xw_x - (1+\lambda)yw_y + \lambda z w_z + \lambda w = -p_z, \tag{2d}$$

where u, v, w and p are the velocity and pressure perturbations, respectively. The appropriate boundary conditions require that all disturbance quantities vanish as $y \rightarrow \infty$ and the normal velocity v is zero on the wall. In addition, the initial conditions consistent with the boundary conditions must be supplied.

The above equations can be recast in terms of the vorticity components $\omega_x, \omega_y, \omega_z$ in the x, y, z directions:

$$\frac{\mathrm{D}\omega_x}{\mathrm{D}t} = \omega_x, \quad \frac{\mathrm{D}\omega_y}{\mathrm{D}t} = -(1+\lambda)\,\omega_y, \quad \frac{\mathrm{D}\omega_z}{\mathrm{D}t} = \lambda\omega_z, \tag{3}$$

where $\mathrm{D}/\mathrm{D}t$ is the linearized material derivative defined by

$$\frac{\mathrm{D}(\,)}{\mathrm{D}t} = (\,)_t + x(\,)_x - (1+\lambda)y(\,)_y + \lambda z(\,)_z. \tag{4}$$

In general, only two vorticity components can be specified at time $t = 0$; the third component is found by appealing to the fact that vorticity must be solenoidal, given by

$$\frac{\partial \omega_x}{\partial x} + \frac{\partial \omega_y}{\partial y} + \frac{\partial \omega_z}{\partial z} = 0. \tag{5}$$

In this study, the initial profiles for the vorticity components ω_x and ω_z are specified, and (5) is used to determine ω_y. Once the vorticity has been determined from (3), the v velocity component is found by solving

$$\nabla^2 v = \frac{\partial \omega_z}{\partial x} - \frac{\partial \omega_x}{\partial z} \tag{6}$$

subject to appropriate boundary conditions, where ∇^2 is the three-dimensional Laplace

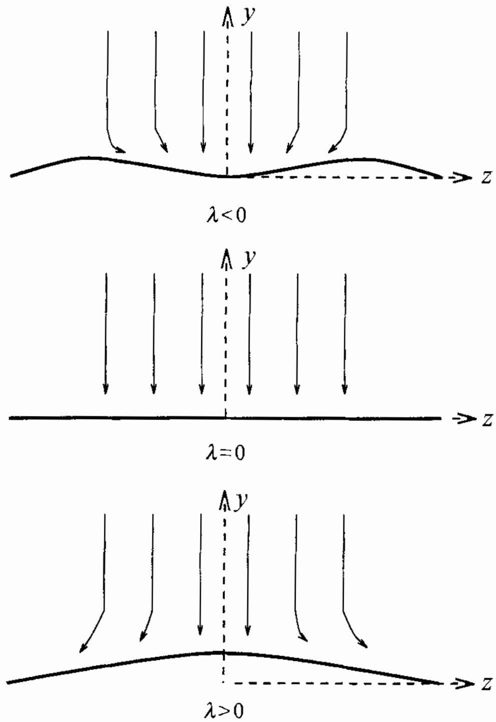

FIGURE 1. Schematic of a cross-section of the three-dimensional stagnation-point flow. Shown are the (w, v)-velocity components in the (z, y)-plane.

operator. The other velocity components are determined by appealing to the vorticity relations together with the continuity equation, yielding

$$\nabla_2^2 u = \frac{\partial \omega_y}{\partial z} - \frac{\partial^2 v}{\partial x \, \partial y}, \tag{7}$$

$$\nabla_2^2 w = -\frac{\partial \omega_y}{\partial x} - \frac{\partial^2 v}{\partial y \, \partial z}, \tag{8}$$

where ∇_2^2 is the two-dimensional Laplace operator in the (x, z)-plane.

By following Criminale & Drazin (1990), an analytical solution is readily obtained if a change from an Eulerian to a moving coordinate system is made. The moving-coordinate transformation

$$\xi = x\,\mathrm{e}^{-t}, \quad \eta = y\,\mathrm{e}^{(1+\lambda)\,t}, \quad \zeta = z\,\mathrm{e}^{-\lambda t}, \quad T = t \tag{9}$$

is chosen so that the system of equations (3) have coefficients that are functions of time only and the material derivative (4) becomes

$$\frac{\mathrm{D}(\,)}{\mathrm{D}t} = \frac{\partial(\,)}{\partial T}. \tag{10}$$

The notable feature of this transformation is that the partial differential equations for the individual vorticity components (3) can then be immediately integrated in time and the solutions are

$$\omega_x = \omega_x^0\,\mathrm{e}^{T}, \quad \omega_y = \omega_y^0\,\mathrm{e}^{-(1+\lambda)\,T}, \quad \omega_z = \omega_z^0\,\mathrm{e}^{\lambda T}, \tag{11}$$

where the superscript 0 denotes the specified values at $T = 0$. Once the initial values ω_x^0 and ω_z^0 have been found, the initial value of ω_y^0 is determined from the conservation of vorticity (equation (5)). The equation for the v velocity component in the moving coordinates is

$$\Delta v = \mathrm{e}^{-(1-\lambda)T}\frac{\partial \omega_z^0}{\partial \xi} - \mathrm{e}^{(1-\lambda)T}\frac{\partial \omega_x^0}{\partial \zeta}, \tag{12}$$

where Δ is the Laplace operator in the moving coordinates, namely

$$\Delta = \mathrm{e}^{-2T}\frac{\partial^2}{\partial \xi^2} + \mathrm{e}^{2(1+\lambda)T}\frac{\partial^2}{\partial \eta^2} + \mathrm{e}^{-2\lambda T}\frac{\partial^2}{\partial \zeta^2}. \tag{13}$$

It is noted that the time dependence in (12) appears as a parameter only and hence finding a solution to (12) is essentially a spatial problem. The equations for the other two velocity components in the moving coordinate system are

$$\Delta_2 u = \mathrm{e}^{-(1+2\lambda)T}\frac{\partial \omega_y^0}{\partial \zeta} - \mathrm{e}^{\lambda T}\frac{\partial^2 v}{\partial \xi \partial \eta}, \tag{14}$$

$$\Delta_2 w = -\mathrm{e}^{-(2+\lambda)T}\frac{\partial \omega_y^0}{\partial \xi} - \mathrm{e}^{T}\frac{\partial^2 v}{\partial \zeta \partial \eta}, \tag{15}$$

where

$$\Delta_2 = \mathrm{e}^{-2T}\frac{\partial^2}{\partial \xi^2} + \mathrm{e}^{-2\lambda T}\frac{\partial^2}{\partial \zeta^2} \tag{16}$$

is the two-dimensional Laplace operator in the moving system.

It is now assumed that Fourier transforms may be taken in the ξ- and ζ-directions, which implies that the disturbances are bounded in these directions. The double Fourier transform is defined by

$$\hat{u}(\alpha, \eta, \gamma, T) = \iint_{-\infty}^{\infty} u(\xi, \eta, \zeta, T)\,\mathrm{e}^{\mathrm{i}(\alpha\xi+\gamma\zeta)}\,\mathrm{d}\xi\,\mathrm{d}\zeta, \tag{17}$$

etc. for $\hat{v}$, $\hat{w}$, $\hat{p}$, $\hat{\omega}$ with the inversion given by

$$u(\xi, \eta, \zeta, T) = \frac{1}{(2\pi)^2}\iint_{-\infty}^{\infty} \hat{u}(\alpha, \eta, \gamma, T)\,\mathrm{e}^{-\mathrm{i}(\alpha\xi+\gamma\zeta)}\,\mathrm{d}\alpha\,\mathrm{d}\gamma. \tag{18}$$

The transforms of the relevant equations are

$$\mathrm{e}^{2(1+\lambda)T}\frac{\partial^2 \hat{v}}{\partial \eta^2} - \tilde{\alpha}^2\hat{v} = -\mathrm{i}\alpha\hat{\omega}_z^0\,\mathrm{e}^{-(1-\lambda)T} + \mathrm{i}\gamma\hat{\omega}_x^0\,\mathrm{e}^{(1-\lambda)T}, \tag{19}$$

$$\frac{\partial \hat{\omega}_y^0}{\partial \eta} = \mathrm{i}\alpha\hat{\omega}_x^0 + \mathrm{i}\gamma\hat{\omega}_z^0, \tag{20}$$

$$\hat{u} = \frac{1}{\tilde{\alpha}^2}\left[\mathrm{i}\gamma\hat{\omega}_y^0\,\mathrm{e}^{-(1+2\lambda)T} - \mathrm{i}\alpha\frac{\partial \hat{v}}{\partial \eta}\mathrm{e}^{\lambda T}\right], \tag{21}$$

$$\hat{w} = \frac{1}{\tilde{\alpha}^2}\left[-\mathrm{i}\alpha\hat{\omega}_y^0\,\mathrm{e}^{-(2+\lambda)T} - \mathrm{i}\gamma\frac{\partial \hat{v}}{\partial \eta}\mathrm{e}^{T}\right], \tag{22}$$

with

$$\tilde{\alpha}^2 = \alpha^2\mathrm{e}^{-2T} + \gamma^2\mathrm{e}^{-2\lambda T}. \tag{23}$$

The equation for $\hat{v}$ is a second-order ordinary differential equation in η with time-dependent coefficients, and since $\tilde{\alpha}^2$ is just the Fourier transform of Δ_2, the velocity components $\hat{u}$ and $\hat{w}$ are determined directly from the algebraic relations provided by transforming (14) and (15).

The evolution of a single Fourier mode can be studied by choosing the initial conditions for the vorticity components ω_x^0 and ω_z^0 to be

$$(\omega_x^0, \omega_z^0) = (\Omega_x, \Omega_z)\,\mathrm{e}^{-\mathrm{i}(\alpha_0\xi+\gamma_0\zeta)}\delta(\eta-y_0) \tag{24}$$

since $(x, y, z) = (\xi, \eta, \zeta)$ at $T = 0$. In Fourier space,

$$(\hat{\omega}_x^0, \hat{\omega}_z^0) = (\Omega_x, \Omega_z)\,\delta(\alpha-\alpha_0)\,\delta(\gamma-\gamma_0)\,\delta(\eta-y_0). \tag{25}$$

The initial value for the last vorticity component is found by transforming (20) and integrating in the η-direction:

$$\hat{\omega}_y^0 = (\mathrm{i}\alpha\Omega_x + \mathrm{i}\gamma\Omega_z)\,\delta(\alpha-\alpha_0)\,\delta(\gamma-\gamma_0)\,[H(\eta-y_0)-1], \tag{26}$$

where $H(\eta)$ is the step function. The constant of integration has been chosen so that all of the velocity components vanish as $\eta \to \infty$.

With the vorticity components known, the differential equation for $\hat{v}$ is integrated, and

$$\hat{v} = \frac{\mathrm{e}^{(1+\lambda)T}}{2\tilde{\alpha}}\{\mathrm{i}\alpha\Omega_z\,\mathrm{e}^{-(3+\lambda)T} - \mathrm{i}\gamma\Omega_x\,\mathrm{e}^{-(1+3\lambda)T}\}\,\delta(\alpha-\alpha_0)\,\delta(\gamma-\gamma_0)$$
$$\times\{\exp[-\tilde{\alpha}\,\mathrm{e}^{-(1+\lambda)T}|\eta-y_0|] - \exp[-\alpha\,\mathrm{e}^{-(1+\lambda)T}(\eta+y_0)]\}, \tag{27}$$

where $\tilde{\alpha}$ is as defined earlier. The solution decays as $\eta \to \infty$ and is zero at the wall. Once the transform is inverted, the velocity component is given by

$$v(\xi, \eta, \zeta, T) = \frac{1}{2(2\pi)^2\tilde{\alpha}_0}\{\mathrm{i}\alpha_0\,\Omega_z\,\mathrm{e}^{-2T} - \mathrm{i}\gamma_0\,\Omega_x\,\mathrm{e}^{-2\lambda T}\}\,\mathrm{e}^{-\mathrm{i}(\alpha_0\xi+\gamma_0\zeta)}$$
$$\times\{\exp[-\tilde{\alpha}_0\,\mathrm{e}^{-(1+\lambda)T}|\eta-y_0|] - \exp[-\tilde{\alpha}_0\,\mathrm{e}^{-(1+\lambda)T}(\eta+y_0)]\} \tag{28}$$

where

$$\tilde{\alpha}_0^2 = a_0^2\,\mathrm{e}^{-2T} + \gamma_0^2\,\mathrm{e}^{-2\lambda T}. \tag{29}$$

The u- and w-components are determined directly from the earlier equations and, upon inverting the transforms, these components are found to be

$$u(\xi, \eta, \zeta, T) = \frac{-\gamma_0}{(2\pi)^2\tilde{\alpha}_0^2}[\alpha_0\,\Omega_x + \gamma_0\,\Omega_z]\,\mathrm{e}^{-(1+2\lambda)T}\,\mathrm{e}^{-\mathrm{i}(\alpha_0\xi+\gamma_0\zeta)}[H(\eta-y_0)-1]$$
$$-\frac{\alpha_0}{2(2\pi)^2\tilde{\alpha}_0^2}\{\alpha_0\,\Omega_z\,\mathrm{e}^{-3T} - \gamma_0\,\Omega_x\,\mathrm{e}^{-(1+2\lambda)T}\}\,\mathrm{e}^{-\mathrm{i}(\alpha_0\xi+\gamma_0\zeta)}$$
$$\times\{\operatorname{sign}(\eta-y_0)\exp[-\tilde{\alpha}_0\,\mathrm{e}^{-(1+\lambda)T}|\eta-y_0|] - \exp[-\tilde{\alpha}_0\,\mathrm{e}^{-(1+\lambda)T}(\eta+y_0)]\}, \tag{30}$$

and

$$w(\xi, \eta, \zeta, T) = \frac{\alpha_0}{(2\pi)^2\tilde{\alpha}_0^2}[\alpha_0\,\Omega_x + \gamma_0\,\Omega_z]\,\mathrm{e}^{-(2+\lambda)T}\,\mathrm{e}^{-\mathrm{i}(\alpha_0\xi+\gamma_0\zeta)}[H(\eta-y_0)-1]$$
$$-\frac{\gamma_0}{2(2\pi)^2\tilde{\alpha}_0^2}\{\alpha_0\,\Omega_z\,\mathrm{e}^{-2(2+\lambda)T} - \gamma_0\,\Omega_x\,\mathrm{e}^{-3\lambda T}\}\,\mathrm{e}^{-\mathrm{i}(\alpha_0\xi+\gamma_0\zeta)}$$
$$\times\{\operatorname{sign}(\eta-y_0)\exp[-\tilde{\alpha}_0\,\mathrm{e}^{-(1+\lambda)T}|\eta-y_0|] - \exp[-\tilde{\alpha}_0\,\mathrm{e}^{-(1+\lambda)T}(\eta+y_0)]\}. \tag{31}$$

3. Single mode: infinite wave train

In this section we present selected results for the single-mode solutions given above for u, v, and w. We first note that the solutions are a linear combination of Ω_x and Ω_z. Therefore, there exist two modes, defined as follows:

Mode I: $\Omega_x = 0, \quad \Omega_z = 1;$

Mode II: $\Omega_x = 1, \quad \Omega_z = 0.$

The results for Mode I are shown in figure 2 for three values of the wavenumber in the z-direction ($\gamma_0 = 0$, 0.1, and 1.0) and a single value of the wavenumber in the x-direction ($\alpha_0 = 1.0$). Plotted in this figure is the maximum amplitude of the velocity components $|u|_{max}$, $|v|_{\max}$, and $|w|_{max}$ as a function of time. The maximum in the u- and w-velocities are at the wall, while the maximum in the v-velocity is in the interior for all times since it is required that v vanish at the wall. In each part of the figure, four values of the three-dimensionality constant were chosen: axisymmetric flow, $\lambda = 1$ (shown in the figures as a small-dashed curve); $\lambda = 0.5$; planar stagnation-point flow, $\lambda = 0$ (shown in the figures as a large-dashed curve); and $\lambda = -0.2$.

Included in this figure are the results for the special cases of two-dimensional disturbances in a two-dimensional flow ($\gamma_0 = 0, \lambda = 0$), two-dimensional disturbances in a three-dimensional flow ($\gamma_0 = 0, \lambda \neq 0$), and three-dimensional disturbances in a two-dimensional flow ($\gamma_0 \neq 0, \lambda = 0$).

As seen from the figure, all three components of the flow exhibit exponential decay in the long-time solution for the response of this mode. The results for the u-velocity show that the decay rate is independent of the variable λ and of the wavenumber in the z-direction. Since the analytic solution for the velocities is known, this information can be found by determining the behaviour of (30) as $T \rightarrow \infty$ and is

$$u(\xi, 0, \zeta, T) = \frac{1}{(2\pi)^2} \mathrm{e}^{-T} \mathrm{e}^{-\mathrm{i}(\alpha_0 \xi + \gamma_0 \zeta)}, \tag{32}$$

where the first term of (30) is dominant when $\lambda < 1$, and there is a balance between the first and second terms for the axisymmetric case $\lambda = 1$ that does not, however, change the limit. For the long-time behaviour of the v-component of the velocity the maximum must be determined. The maximum is found to always occur at $\eta = y_0$ so that

$$v(\xi, y_0, \zeta, T) = \frac{\mathrm{i}\alpha_0 y_0}{(2\pi)^2} \mathrm{e}^{-(3+\lambda)T} \mathrm{e}^{-\mathrm{i}(\alpha_0 \xi + \gamma_0 \zeta)} \tag{33}$$

with the axisymmetric case again being a special limit that does affect the amplitude in the above equation but not the decay rate. The asymptotic behaviour for the w-component of the velocity is also determined analytically. From (31) it is found that

$$w(\xi, 0, \zeta, T) = -\frac{\alpha_0 \gamma_0 y_0}{(2\pi)^2 |\gamma_0|} \mathrm{e}^{-(3+\lambda)T} \mathrm{e}^{-\mathrm{i}(\alpha_0 \xi + \gamma_0 \zeta)}. \tag{34}$$

The dependence of the decay rate of the v- and w-components on the three-dimensionality parameter λ is clearly seen in figure 2.

Although the above analytic forms appear to be relatively simple, the use of the transformed variables ζ, ξ and η tend to hide some rather significant changes in the spatial structure of the disturbances. For $\lambda > 0$ there is a stretching of the initial Fourier-mode form in both the x-direction and the z-direction. For the axisymmetric case, this stretching occurs at an equal rate in both directions. For the planar

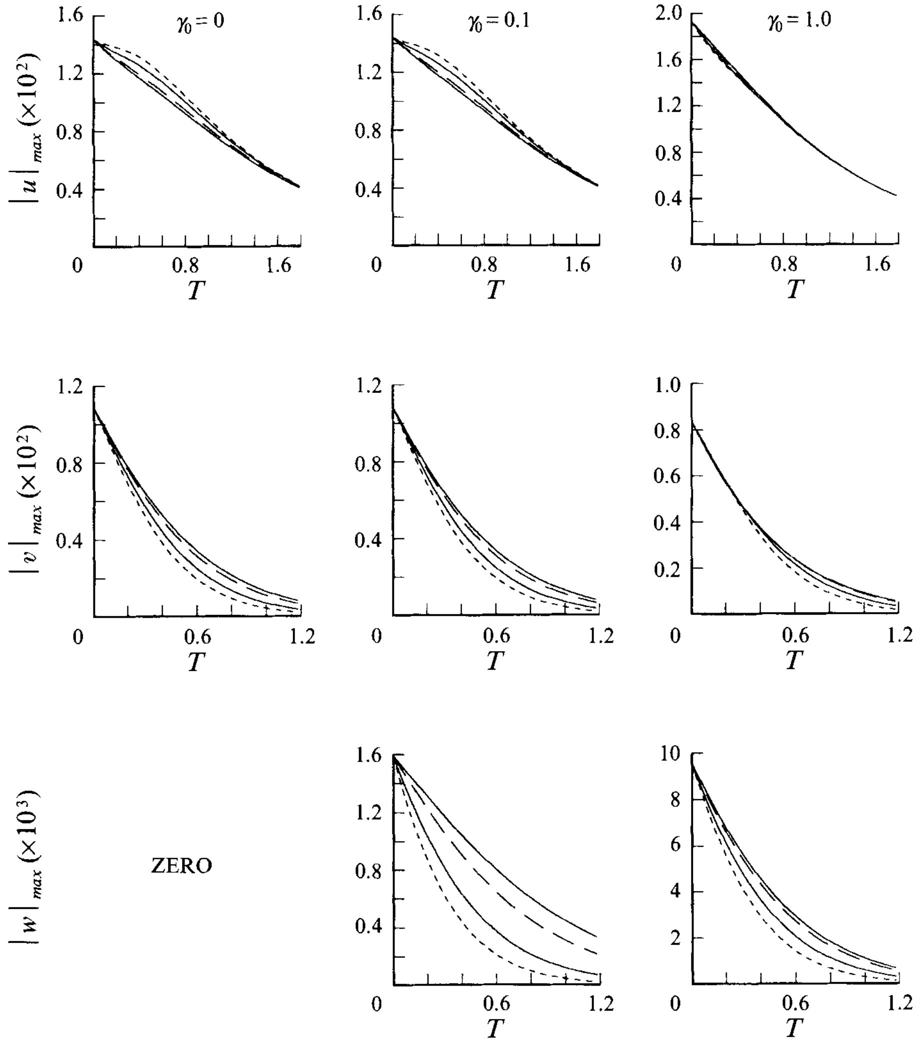

FIGURE 2. Maximum amplitude of the velocity components as a function of time for Mode I disturbances for three values of the z-wavenumber. In each part, four values of the three-dimensionality constant are chosen: axisymmetric flow, $\lambda = 1$ (shown in the figures as a small-dashed curve); $\lambda = 0.5$; planar stagnation-point flow, $\lambda = 0$ (shown in the figures as a large-dashed curve); and $\lambda = -0.2$.

stagnation-point flow $\lambda = 0$ there is no stretching of the disturbance in the z-direction, and for $\lambda < 0$ where the mean flow is towards the stagnation point in the z-direction, there is a contraction of the initial Fourier-mode form in the z-direction. In the y-direction, it is noted that although the maximum in v-velocity is at a fixed value of η, this implies that this maximum approaches the wall exponentially fast when the problem is converted to the physical spatial variables, that is the inverse of (9).

Although the long-time behaviour of the disturbances is of course very important, equally important is the transient evolution since it is possible for there to be significant initial growth (or perhaps a long-time persistence) of the disturbance quantities before the inevitable exponential decay. By examining the results of figure 2, it is seen that the initial response to a Mode I disturbance is typically a linear decay in time. The initial

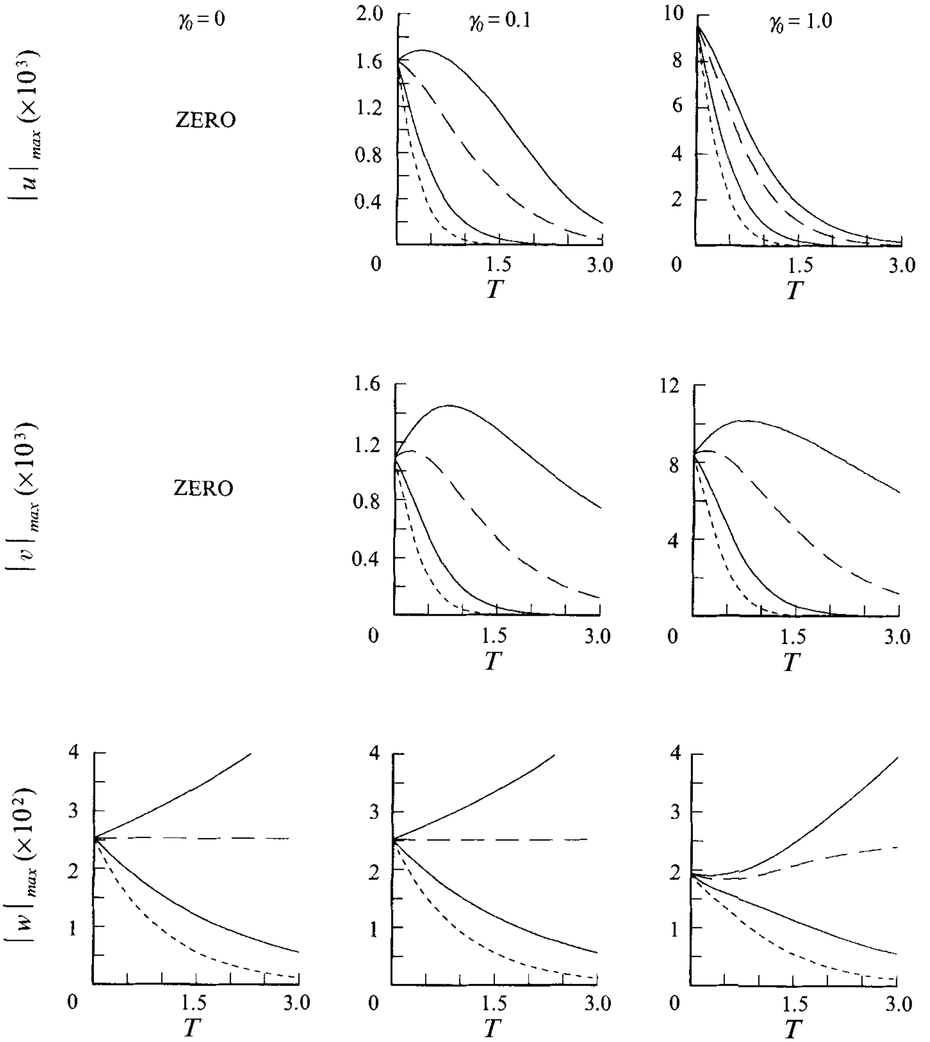

FIGURE 3. As figure 2 but for Mode II disturbances.

linear decay rate depends on the value of the three-dimensionality parameter λ with $\lambda < 0$ decaying at the slowest rate. The λ-dependence of this initial decay rate is strongest for smaller wavenumbers in the z-direction.

The results for the single-mode response to a Mode II disturbance are shown in figure 3. A significant difference from the Mode I results is immediately noticeable. Analytically the long-time limits are given by

$$u(\xi, 0, \zeta, T) = \frac{\alpha_0 \gamma_0 y_0}{(2\pi)^2 |\gamma_0|} \mathrm{e}^{-2(1+\lambda)T} \mathrm{e}^{-\mathrm{i}(\alpha_0 \xi + \gamma_0 \zeta)}, \tag{35}$$

$$v(\xi, y_0, \zeta, T) = -\frac{\mathrm{i}\gamma_0 y_0}{(2\pi)^2} \mathrm{e}^{-(1+3\lambda)T} \mathrm{e}^{-\mathrm{i}(\alpha_0 \xi + \gamma_0 \zeta)}, \tag{36}$$

and

$$w(\xi, 0, \zeta, T) = -\frac{1}{(2\pi)^2} \mathrm{e}^{-\lambda T} \mathrm{e}^{-\mathrm{i}(\alpha_0 \xi + \gamma_0 \zeta)}, \tag{37}$$

as $T \to \infty$. It is seen from figure 3 that the u- and v-components of velocity decay

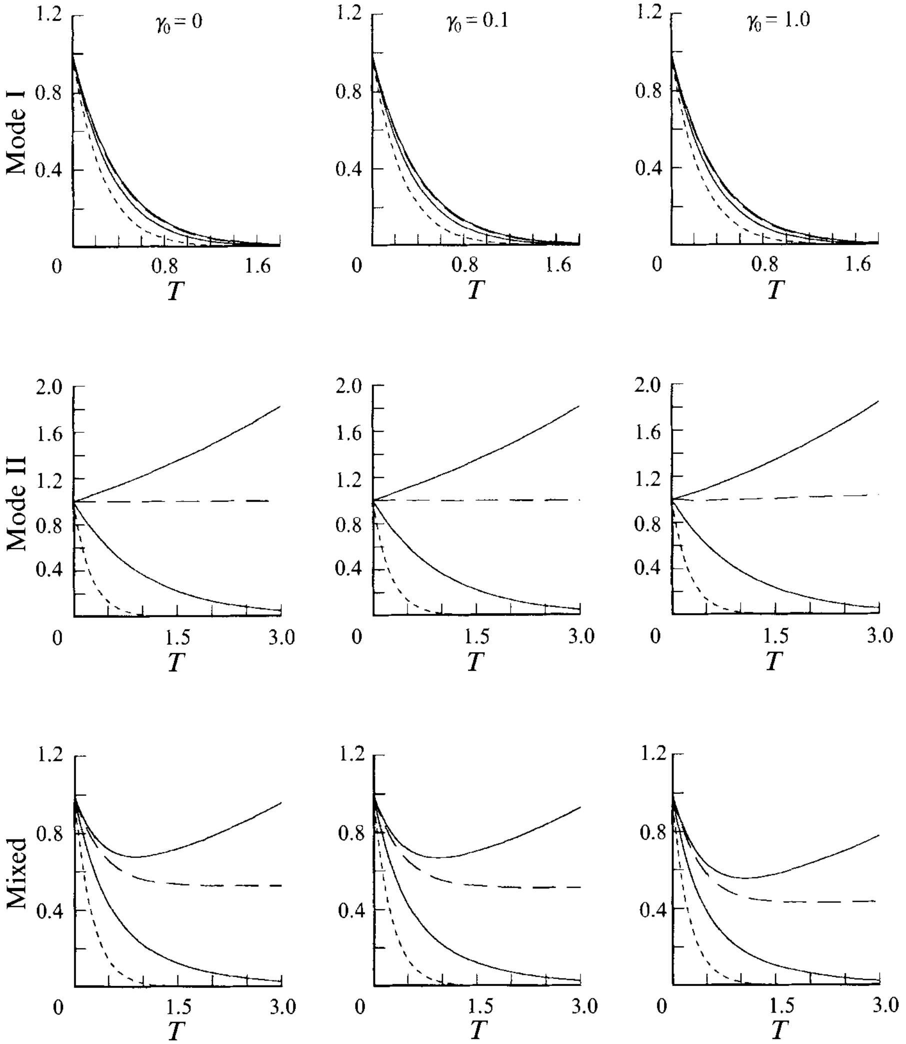

FIGURE 4. Normalized energy E as a function of time. In each part, four values of the three-dimensionality constant are chosen: axisymmetric flow, $\lambda = 1$ (shown in the figures as a small-dashed curve); planar stagnation-point flow, $\lambda = 0$; $\lambda = -\frac{1}{3}$ (shown in the figures as a large-dashed curve); and $\lambda = -0.4$.

exponentially for all λ while the w-component of velocity only decays when the three-dimensionality parameter λ is greater than zero. This value of λ corresponds to a stretching of the original disturbance in the z-direction. However, for the planar stagnation-point flow where $\lambda = 0$ the w-component approaches a constant independent of the initial wavenumber in the x- and z-directions. For the case where there is mean flow towards the stagnation point along the z-direction ($\lambda < 0$), the w-component grows exponentially. It is seen that the initial behaviour of the u- and v-components also reflects this differing behaviour for the planar stagnation-point flow and the $\lambda < 0$ case. It is also true that there is initially linear growth of these components. As in the Mode I case, the dependence of the behaviour for early time on the three-dimensionality parameter is strongest at smaller wavenumbers in the z-direction.

The results presented in figures 2 and 3 give the maximum values of the velocities, but considering the severe contraction of the disturbances in the y-direction, as evidenced by the movement of the maximum in the v-velocity toward the wall at an exponentially fast rate, it is perhaps more useful to look at the growth or decay of the energy of the disturbances. For the single-Fourier-mode results presented in this section, it is necessary to consider the energy per period in the ξ- and ζ-directions, or equivalently the energy per period in the x- and z-directions. Because of the stretching in the x-direction and the stretching or contraction (depending on the sign of λ) in the z-direction, these results do not readily lend themselves to direct physical interpretation; however, they do help point out the effect that the contraction has in the vertical direction y. Shown in figure 4 as a function of time is the quantity E defined by

$$E(t) = \frac{1}{2}\int_0^\infty [|u|^2+|v|^2+|w|^2]\,\mathrm{d}y, \tag{38}$$

where u, v, and w are given by (28), (30), and (31). Each graph was normalized by the value at time $t = 0$. The amplitudes Ω_x and Ω_z are equal in the mixed-mode results. In each part of the figure, four values of the three-dimensionality constant were chosen: axisymmetric flow, $\lambda = 1$ (shown in the figures as a small-dashed curve); planar stagnation-point flow, $\lambda = 0$; $\lambda = -\frac{1}{3}$ (shown in the figures as a large-dashed curve); and λ; $= -0.4$. From these figures, Mode II is seen to represent disturbances that may grow in energy as it also represented disturbances with growth in the maximum values of the velocities. However, it is noted that although the maximum in the velocities can grow for any $\lambda < 0$, the energy per period grows only for $\lambda < -\frac{1}{3}$. This phenomenon is directly related to the contraction in the y-direction. Very little dependence on the wavenumber in the z-direction can be detected, which is consistent with the results of figures 2 and 3. The energy of Mode I is dominated by the u- and v-velocities, which show little dependence on γ_0, and the Mode II energy is dominated by the w-velocity, which also shows little dependence on γ_0.

4. Finite wave packet

In the previous section, the results for an initial disturbance that consisted of a single Fourier mode were presented. This disturbance has an infinite spatial profile in the (x, z)-plane. Considering the distortions in the x- and z-directions introduced by the transformed variables, there is considerable doubt as to the proper interpretation of the single-mode results. To resolve this difficulty in the analysis, an initial disturbance that is localized in space is chosen. The initial vorticity profile is taken as a Gaussian. The disturbance is initially symmetric in the (x, z)-plane and, since the inviscid problem is being investigated, a Gaussian profile in the y-direction is also chosen and all boundary conditions can still be satisfied.

The analysis proceeds by replacing (24) with

$$(\omega_x^0, \omega_z^0) = \frac{(\Omega_x, \Omega_z)}{(2\pi^3\sigma^2\beta)^{\frac{1}{4}}}\,\mathrm{e}^{-\xi^2+\zeta^2/4\sigma}\,\mathrm{e}^{-\eta^2/4\beta}. \tag{39}$$

In Fourier space,

$$(\hat{\omega}_x^0, \hat{\omega}_z^0) = \frac{4\pi\sigma(\Omega_x, \Omega_z)}{(2\pi^3\sigma^2\beta)^{\frac{1}{4}}}\,\mathrm{e}^{-\sigma(\alpha^2+\gamma^2)}\,\mathrm{e}^{-\eta^2/4\beta}, \tag{40}$$

where the constant is chosen such that the integral of the square of the vorticity over the domain is a constant for each choice of σ and β.

The above initial conditions can be substituted directly into (19) and (20) which can then be solved for $\hat{v}$ and $\hat{\omega}_y^0$, or the previous results for a delta-function initial condition in the y-direction can be integrated over the dummy variable y_0. Either way, the transform of the vorticity ω_y^0 and the v-component of velocity are given by

$$\hat{\omega}_y^0 = -(\mathrm{i}\alpha\Omega_x + \mathrm{i}\gamma\Omega_z)\frac{4\pi\sigma(\pi\beta)^{\frac{1}{2}}}{(2\pi^3\sigma^2\beta)^{\frac{1}{4}}}\mathrm{e}^{-\sigma(\alpha^2+\gamma^2)}\,\mathrm{erfc}\left(\frac{\eta}{2\beta^{\frac{1}{2}}}\right) \tag{41}$$

and

$$\begin{aligned}\hat{v} = {} & (\mathrm{i}\alpha\Omega_z\,\mathrm{e}^{-(3+\lambda)T} - \mathrm{i}\gamma\Omega_x\,\mathrm{e}^{-(1+3\lambda)T})\frac{4\pi\sigma(\pi\beta)^{\frac{1}{2}}}{(2\pi^3\sigma^2\beta)^{\frac{1}{4}}}\mathrm{e}^{-\sigma(\alpha^2+\gamma^2)} \\ & \times\frac{1}{2\tilde{\alpha}}\exp[\beta\tilde{\alpha}^2\,\mathrm{e}^{-2(1+\lambda)T}]\,\mathrm{e}^{(1+\lambda)T}\left[\exp[\tilde{\alpha}\,\mathrm{e}^{-(1+\lambda)T}\eta]\,\mathrm{erfc}\left(\frac{\eta}{2\beta^{\frac{1}{2}}} + \tilde{\alpha}\,\mathrm{e}^{-(1+\lambda)T}\beta^{\frac{1}{2}}\right)\right. \\ & -\exp[-\tilde{\alpha}\,\mathrm{e}^{-(1+\lambda)T}\eta]\,\mathrm{erfc}\left(\frac{\eta}{2\beta^{\frac{1}{2}}} - \tilde{\alpha}\,\mathrm{e}^{-(1+\lambda)T}\beta^{\frac{1}{2}}\right) \\ & \left. +2\exp[-\tilde{\alpha}\,\mathrm{e}^{-(1+\lambda)T}\eta]\,\mathrm{erf}(\tilde{\alpha}\,\mathrm{e}^{-(1+\lambda)T}\beta^{\frac{1}{2}})\right].\end{aligned} \tag{42}$$

The transforms of the u- and w-components are found directly from (21) and (22) and all transforms can be inverted using (18). The long-time behaviour of $\hat{w}$ at the wall for Mode II is given by

$$\hat{w}(0,T) = -\frac{4\pi\sigma(\pi\beta)^{\frac{1}{2}}}{(2\pi^3\sigma^2\beta)^{\frac{1}{4}}}\mathrm{e}^{-\sigma(\alpha^2+\gamma^2)}\,\mathrm{e}^{-\lambda T} \tag{43}$$

as $T\rightarrow\infty$ which shows that the transform grows exponentially for λ negative, consistent with the results of the single mode.

In order to examine the true behaviour of the evolution to this initially localized disturbance, the energy as a function of time is computed. The energy in terms of the unstretched variables is

$$E(T) = \frac{1}{2}\int_0^\infty\iint_{-\infty}^{\infty}[u^2+v^2+w^2]\,\mathrm{d}x\,\mathrm{d}z\,\mathrm{d}y, \tag{44}$$

which can also be given in terms of integrals over the Fourier-transform quantities in the stretched variables as

$$E(T) = \frac{\mathrm{e}^{(1+\lambda)T}}{8\pi^2}\int_0^\infty\iint_{-\infty}^{\infty}Q^2(\tilde{\alpha}\,\mathrm{e}^{T},\tilde{\gamma}\,\mathrm{e}^{\lambda T},y\,\mathrm{e}^{(1+\lambda)T},T)\,\mathrm{d}\tilde{\alpha}\,\mathrm{d}\tilde{\gamma}\,\mathrm{d}y, \tag{45}$$

where

$$Q^2(\alpha,\gamma,\eta,T) = \hat{u}^2+\hat{v}^2+\hat{w}^2. \tag{46}$$

The normalized energy of the response to a Mode II Gaussian profile with $\beta = 1.0$ and $\sigma = 0.5$ is shown in figure 5 for eight values of the three-dimensionality parameter λ ranging from $\lambda = 1$ (the axisymmetric case) to $\lambda = -0.4$ (near separation). A number of interesting features are noticeable. First, for the planar stagnation-point flow ($\lambda = 0$), the energy approaches a constant value approximately three times the initial value. This is in agreement with the results tracking the maximum in the velocities. The mean flow produces a contraction of the disturbance in the y-direction, initially increasing the magnitude of the w-velocity at the wall and initially increasing the energy of the disturbance. However, a balance develops between the continued contraction in the y-direction and the expansion of the flow in the x-direction thereby leading to the

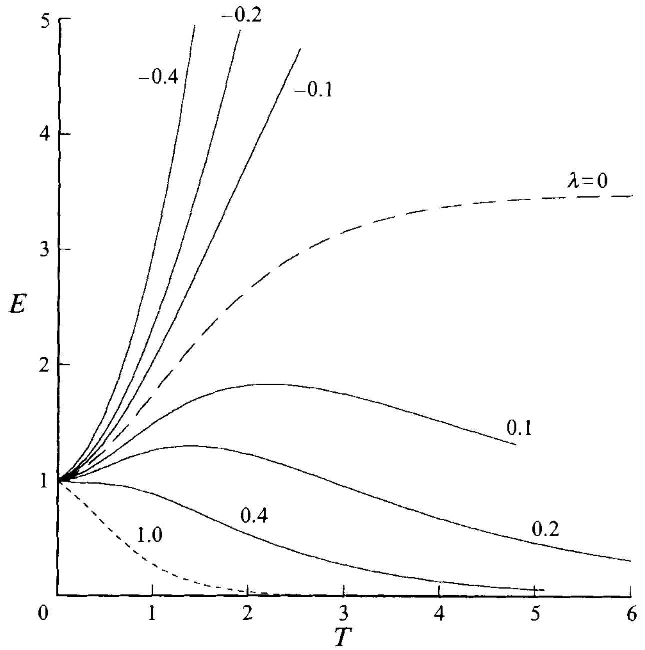

FIGURE 5. Normalized energy of the response to a Mode II Gaussian profile with $\beta = 1.0$ and $\sigma = 0.5$ as a function of time for various values of the three-dimensionality parameter λ.

situation where the energy approaches a constant. This behaviour of the disturbance energy for the two-dimensional planar counter-flow was also seen by Farrell (1989). The purpose of this study is to determine the effects of the three-dimensionality of the mean flow. When these three-dimensional effects are considered ($\lambda \neq 0$), it is seen that the planar stagnation-point flow represents a special case. For λ slightly positive, there is again an initial transient growth in energy. The extra expansion of the flow in the z-direction means that the balance that developed for the planar stagnation-point flow does not develop and the energy of the disturbance eventually decays to zero. For λ sufficiently large and positive there is no initial transient growth, implying that the expansion of the flow in the z-direction is sufficient to prevent the initial increase in disturbance energy. From figure 5, it is seen that for the special case of axisymmetric flow ($\lambda = 1$), the energy undergoes an immediate exponential decay. For λ less than zero, an unstable situation develops, and the energy of the disturbance continually increases at an exponential rate owing to the contraction in both the y- and z-directions which is not balanced by the expansion in the x-direction.

It is also interesting to examine the behaviour of the vorticity components, which are given by (11) in the transformed coordinates. In the physical coordinates, the vorticity field is undergoing a contraction in the y-direction, an expansion in the x-direction and an expansion (for $\lambda > 0$) or a contraction (for $\lambda < 0$) in the z-direction. The exponential time factors in (11) indicate that for a Mode II disturbance, vorticity is transferred from the y-component to the x-component while the transfer of vorticity between the y- and z-components for a Mode I disturbance depends on the sign of λ. By considering the response of a Mode II initial disturbance, it is seen that in the neutrally stable case ($\lambda = 0$) the decay rate of the y-vorticity component is equal to the growth rate of the x-vorticity component. For the stable case ($\lambda > 0$), the decay rate of the y-vorticity component is greater than the growth rate of the x-vorticity component; whereas, for the unstable case ($\lambda < 0$), the decay rate of the y-vorticity component is less than the growth rate of the x-vorticity component. For the Mode I disturbance, either both components are decaying ($\lambda < 0$), or the decay rate of the y-vorticity component is always greater than the growth rate of the z-vorticity component. Perhaps this is an indication of why it is the Mode II disturbances that experience unstable energy growth rather than those of Mode I.

5. Constant-pressure boundary condition

One problem of interest in geophysical fluid dynamics is the case where there is a constant-pressure surface in lieu of a condition on the velocity. Such a problem has been examined by Eady (1949), for example, where plane Couette flow is mathematically equivalent when the constant-pressure surface is used. Consider $p = 0$ at $y = 0$ rather than the v-velocity. Of course the surface $y = 0$ can no longer be thought of as a solid wall. To derive an equation which governs the time evolution of the pressure, the momentum equations (2b) and (2c) can be combined with the continuity equation (2a) in the (ζ, η, ξ, T) coordinate system to get

$$\Delta_2 p = 2(\lambda - 1)\,\mathrm{e}^{-T}\frac{\partial u}{\partial \xi} + \mathrm{e}^{-2\lambda T}\frac{\partial}{\partial T}\left(\mathrm{e}^{(1+3\lambda)T}\frac{\partial v}{\partial \eta}\right), \tag{47}$$

where it is immediately seen that the axisymmetric case $\lambda = 1$ is a special case. In keeping with the previous analysis, the pressure equation is first transformed into Fourier space and then $\hat{u}$ is eliminated by using (21), yielding

$$\tilde{\alpha}^2\hat{p} = -\frac{2\gamma\alpha}{\tilde{\alpha}^2}(\lambda-1)\,\hat{\omega}_y^0\,\mathrm{e}^{-2(1+\lambda)T} + \frac{2\alpha^2}{\tilde{\alpha}^2}(\lambda-1)\,\mathrm{e}^{-(1-\lambda)T}\frac{\partial \hat{v}}{\partial \eta} - \mathrm{e}^{-2\lambda T}\frac{\partial}{\partial T}\left(\mathrm{e}^{(1+3\lambda)T}\frac{\partial \hat{v}}{\partial \eta}\right). \tag{48}$$

If the initial conditions are considered to be given by (24) for this problem so that only a single Fourier mode is investigated, then $\hat{\omega}_y^0$ is given by (26), while (19) can be integrated to find $\hat{v}$, yielding

$$\hat{v} = A_1(T)\exp\left[-\tilde{\alpha}\,\mathrm{e}^{-(1+\lambda)T}|\eta - y_0|\right] + A_2(T)\exp\left[-\tilde{\alpha}\,\mathrm{e}^{-(1+\lambda)T}(\eta - y_0)\right], \tag{49}$$

where
$$A_1(T) = \frac{\mathrm{e}^{(1+\lambda)T}}{2\tilde{\alpha}}\{\mathrm{i}\alpha\Omega_z\,\mathrm{e}^{-(3+\lambda)T} - \mathrm{i}\gamma\Omega_x\,\mathrm{e}^{-(1+3\lambda)T}\}\,\delta(\alpha-\alpha_0)\,\delta(\gamma-\gamma_0). \tag{50}$$

The determination of $A_1(T)$ satisfies all of the conditions at $\eta = y_0$ and it is left to impose the condition on the pressure at $\eta = 0$ in order to determine the remaining unknown function $A_2(T)$. Equation (48) provides the necessary information in determining A_2, but it is convenient to work with an alternative dependent variable defined by

$$B(T) \equiv e^{(1+3\lambda)T}\frac{\partial \hat{v}}{\partial \eta}(0,T) = \tilde{\alpha}\,\mathrm{e}^{2\lambda T}(A_1\exp\left[-\tilde{\alpha}y_0\,\mathrm{e}^{-(1+\lambda)T}\right] - A_2\exp\left[\tilde{\alpha}y_0\,\mathrm{e}^{-(1+\lambda)T}\right]). \tag{51}$$

The equation for $B(T)$ is then

$$\frac{\mathrm{d}B}{\mathrm{d}T} - \frac{2\alpha^2}{\tilde{\alpha}^2}(\lambda-1)\,\mathrm{e}^{-2T}B = -\frac{2\gamma\alpha}{\tilde{\alpha}^2}(\lambda-1)\,\bar{\Omega}\,\mathrm{e}^{-2T}, \tag{52}$$

where
$$\bar{\Omega} = (\mathrm{i}\alpha\Omega_x + \mathrm{i}\gamma\Omega_z)\,\delta(\alpha-\alpha_0)\,\delta(\gamma-\gamma_0). \tag{53}$$

It is helpful to find the long-time solution in order to determine the effects of the three-dimensionality parameter λ. Since Mode II ($\Omega_x = 1, \Omega_z = 0$) is the more interesting initial condition, the rest of the analysis is restricted to this case with $\lambda < 1$. The long-time solution for B is determined directly from (52) or

$$B(T) = B_\infty \bar{\Omega} - \frac{\alpha}{\gamma^2}(\gamma - \alpha\beta_\infty)\bar{\Omega}\,\mathrm{e}^{-2(1-\lambda)T} \tag{54}$$

as $T \to \infty$, where the proportionality to $\bar{\Omega}$ is explicitly given and the constant B_∞ can be found numerically. The behaviour of A_1 is determined directly from (50), and A_2 from (51). These limits are

$$A_1(T) = -\frac{\mathrm{i}}{2}\frac{\gamma}{|\gamma|}\mathrm{e}^{-\lambda T}\delta(\alpha-\alpha_0)\,\delta(\gamma-\gamma_0), \tag{55}$$

$$A_2(T) = -\frac{\mathrm{i}}{|\gamma|}\left(\frac{\gamma}{2} - \alpha B_\infty\right)\mathrm{e}^{-\lambda T}\delta(\alpha-\alpha_0)\,\delta(\gamma-\gamma_0), \tag{56}$$

as $T \to \infty$. The long-time behaviour of the velocities $\hat{u}, \hat{v}, \hat{w}$ is found through (24), (49) and (22), indicating

$$\hat{u}(0,T) = \frac{\alpha}{\gamma^2}(\gamma - \alpha B_\infty)\,\mathrm{e}^{-T}\delta(\alpha-\alpha_0)\,\delta(\gamma-\gamma_0), \tag{57}$$

$$\hat{v}(0,T) = -\frac{\mathrm{i}}{|\gamma|}(\gamma - \alpha B_\infty)\,\mathrm{e}^{-\lambda T}\delta(\alpha-\alpha_0)\,\delta(\gamma-\gamma_0), \tag{58}$$

$$\hat{w}(0,T) = -\frac{\alpha}{\gamma}B_\infty\,\mathrm{e}^{-\lambda T}\delta(\alpha-\alpha_0)\,\delta(\gamma-\gamma_0), \tag{59}$$

as $T \to \infty$. It is seen that, for the boundary condition $p = 0$ on the surface $y = 0$, the velocity components $\hat{v}$ and $\hat{w}$ of Mode II are exponentially growing when the three-dimensionality parameter λ is negative.

6. Effects of background rotation; particle paths

The expression used for the basic velocity and given by (1) can be modified to include effects due to background rotation (strain). Specifically, if Ω_0' is the constant dimensional rate of rotation, then

$$U = x + \Omega_0 z, \quad V = -(1+\lambda)y, \quad W = \lambda z - \Omega_0 x \tag{6}$$

becomes the new non-dimensional representation. The process of shifting to a moving coordinate system and solving for the perturbations as previously done can likewise be accomplished here but with a noticeable increase in complexity. For example, the fundamental vorticity equations (3) used for solving the initial-value problem are no longer uncoupled and the net effect is a higher-order differential system. Thus, the dynamics is altered to some degree. In particular, temporal oscillations become possible but the overall stability conclusions remain. These points can be illustrated by examining the paths of the material particles in the basic flow.

The Cartesian components for any particle in a Lagrangian frame can be written using (60) as

$$\frac{\mathrm{d}x}{\mathrm{d}T} = U = x + \Omega_0 z, \quad \frac{\mathrm{d}y}{\mathrm{d}T} = V = -(1+\lambda)y, \quad \frac{\mathrm{d}z}{\mathrm{d}T} = w = \lambda z - \Omega_0 x. \tag{61 a–c}$$

By assuming $x = x_0$, $y = y_0$ and $z = z_0$ at time $T = 0$, the solutions for (61*a, b, c*) are

$$x = x_0 e^{\sigma T}, \quad y = y_0 e^{-(1+\lambda)T}, \tag{62a, b}$$

$$z = z_0 e^{\lambda T} - \frac{\Omega_0 x_0}{\sigma\lambda}(e^{\sigma T} - e^{\lambda T}), \tag{62c}$$

with

$$\sigma = \frac{1+\lambda}{2}\left(1 + \left(1 - 4\frac{\lambda + \Omega_0^2}{(1+\lambda)^2}\right)^{\frac{1}{2}}\right). \tag{63}$$

Oscillatory solutions are possible if $\Omega_0 > \frac{1}{2}(1-\lambda)$. In general, particles will move arbitrarily far from any initial position.

Two interesting limits of (62*a, b, c*) are when $\Omega_0 = 0$ or $\lambda = 1$; λ can never be very negative and therefore a change in the system behaviour using this parameter is not possible. In the first instance, $\Omega_0 = 0$, then

$$x = x_0 e^{T}, \quad y = y_0 e^{-(1+\lambda)T}, \quad z = z_0 e^{\lambda T}. \tag{64}$$

The novel feature of (65) is that these results are identical to those of (11) for the vorticity, where x, y, z are replaced by $\omega_x, \omega_y, \omega_z$. In short, this is a unique situation where, for a three-dimensional flow, the particle paths are synonymous with vortex lines. Extending this argument to the $\Omega_0 \neq 0$ case can be made by conjecture since the vorticity has not been determined under these circumstances. Thus, there is little likelihood that the instability predictions for the non-rotating case can be changed by a finite Ω_0. When $\lambda = 1$, the basic flow is axisymmetric and $\sigma = 1 + i\Omega_0$, indicating that background rotation acts as a spring force and therefore oscillations in time result.

7. Conclusions

We have investigated the evolution of three-dimensional disturbances in a fully three-dimensional stagnation-point in an inviscid fluid. It has been shown that the planar stagnation-point flow is a special case in which the disturbance energy approaches a constant for long time. If the flow in the second transverse coordinate is away from the stagnation point then the flow expands in the transverse direction such that the disturbance energy decays after an initial transient growth. As the limiting case of axisymmetric flow is approached, the disturbance energy is found to decay without an initial transient growth. For flow towards the stagnation point in the second transverse direction, it is found that the disturbance energy may grow exponentially, thus indicating an unstable flow configuration. These results were found by determining a closed-form solution to the initial value problem even though a classical mode analysis was not possible for the fully three-dimensional flow.

Because of the inviscid assumption, the results for the planar stagnation-point flow cannot be compared directly with previous work but the method used here can be extended (with considerably more mathematical complexity) to the study of the inviscid mean flow subject to viscous linear disturbances. These results can be compared with some of the previous work. However, any results for this problem can only be suggestive in view of the fact that the basic flow is derived from an inviscid basis. Using normal-mode analysis, Wilson & Gladwell (1978) and Lyell & Huerre (1985) show that viscous disturbance modes of the inviscid planar stagnation-point flow are stable. The work of Hall *et al.* (1984) shows that the addition of a third velocity component of sufficient strength can destabilize the viscous normal modes. This suggests that the three-dimensionality considered here might also overcome the stabilizing effects of viscosity.

Background rotation or strain of the field can only alter the dynamics by forcing the system to have temporal oscillations rather than prevent instabilities. Finally, more comprehensive material particle-path information could be obtained if one allows the velocity field to include the perturbations as well as the basic flow. Pursuit of this information will involve three-dimensional coupled nonlinear non-autonomous differential equations.

This work was supported, in part, by the National Aeronautics and Space Administration under NASA Contract NAS1-19480 while the authors were in residence at the Institute for Computer Applications in Science and Engineering, NASA Langley Research Center, Hampton, VA 23681. T.L.J. also acknowledges support by the AFOSR under contract 91-0180.

REFERENCES

BRATTKUS, K. & DAVIS, S. H. 1991 The linear stability of plane stagnation-point flow against general disturbances. *Q. J. Mech. Appl. Maths* **44**, 135–146.

CRIMINALE, W. O. & DRAZIN, P. G. 1990 The evolution of linearized perturbations of parallel flows. *Stud. Appl. Maths* **83**, 123–157.

DAVEY, A. 1961 Boundary-layer flow at a saddle point of attachment. *J. Fluid Mech.* **38**, 593–610.

EADY, E. A. 1949 Long waves and cyclone waves. *Tellus* **1**, 33–52.

FARRELL, B. F. 1989 Transient development in confluent and diffluent flow. *J. Atmos. Sci.* **46**, 3279–3288.

HALL, P., MALIK, M. R. & POLL, D. I. A. 1984 On the stability of an infinite swept attachment line boundary layer. *Proc. R. Soc. Lond.* A **395**, 229–245.

KAZAKOV, A. V. 1991 Effect of surface temperature on the stability of the swept attachment line boundary layer. *Fluid Dyn.* **25**, 875–878.

KELVIN, W. 1887 Rectilinear motion of viscous fluid between two parallel plates. *Phil. Mag.* **24**, 188–196.

LASSEIGNE, D. G. & JACKSON, T. L. 1992 Stability of a non-orthogonal stagnation flow to three dimensional disturbances. *Theor. Comput. Fluid Dyn.* **3**, 207–218.

LASSEIGNE, D. G., JACKSON, T. L. & HU, F. Q. 1992 Temperature and suction effects on the instability of an infinite swept attachment line. *Phys. Fluids* A **4**, 2008–2012.

LYELL, M. J. & HUERRE, P. 1985 Linear and nonlinear stability of plane stagnation flow. *J. Fluid Mech.* **161**, 295–312.

ORR, W. M'F. 1907*a* The stability or instability of the steady motions of a perfect liquid and a viscous liquid. Part I. *Proc. R. Irish Acad.* **27**, 9–68.

ORR, W. M'F. 1907*b* The stability or instability of the steady motions of a perfect liquid and a viscous liquid. Part II. *Proc. R. Irish Acad.* **27**, 69–138.

SPALART, P. R. 1989 Direct numerical study of leading-edge contamination. *AGARD Conf. Proc.* **438**, 5.1–5.13.

WILSON, S. D. R. & GLADWELL, I. 1978 The stability of a two-dimensional stagnation flow to three-dimensional disturbances. *J. Fluid Mech.* **84**, 517–527.